Am J Physiol Lung Cell Mol Physiol 328: L430–L442, 2025.
First published October 22, 2024; doi:10.1152/ajplung.00305.2023

american physiological society

AMERICAN JOURNAL OF PHYSIOLOGY
LUNG CELLULAR AND MOLECULAR PHYSIOLOGY

RESEARCH ARTICLE

Translational Physiology

Enhanced lung endothelial glycolysis is implicated in the development of severe pulmonary hypertension in type 2 diabetes

Qiuyu Zheng,[1,2]* Jody Tori O. Cabrera,[1]* Atsumi Tsuji-Hosokawa,[3]* Francisco J. Ramirez,[4] Hua Cai,[5] Jason X. -J. Yuan,[1] Jian Wang,[1,6] and Ayako Makino[1,3,4]

[1]*Department of Medicine, University of California, San Diego, La Jolla, California, United States;* [2]*Department of Pulmonary and Critical Care Medicine, The Second Affiliated Hospital of Guangzhou Medical University, Guangzhou, China;* [3]*Department of Physiology, University of Arizona, Tucson, Arizona, United States;* [4]*Center for Inflammation Science and Systems Medicine, The Herbert Wertheim University of Florida/Scripps Institute for Biomedical Innovation & Technology, Jupiter, Florida, United States;* [5]*Department of Anesthesiology, University of California, Los Angeles, Los Angeles, California, United States; and* [6]*State Key Laboratory of Respiratory Disease, Guangzhou Institute of Respiratory Disease, The First Affiliated Hospital of Guangzhou Medical University, Guangzhou, China*

Abstract

Metabolic abnormalities in pulmonary endothelial cells are implicated in pulmonary hypertension (PH) while increasing evidence shows the influence of diabetes on progressing PH. In this study, we examined the effect of type 2 diabetes on hypoxia-induced PH and investigated its molecular mechanisms using hypoxia-induced diabetic male mice. Chronic hypoxia led to a more severe PH in type 2 diabetic mice than in control mice. Next, we compared gene expression patterns in isolated pulmonary endothelial cells (MPECs) from control mice in normoxia (CN), diabetic mice in normoxia (DN), control mice exposed to hypoxia (CH), and diabetic mice exposed to hypoxia (DH). The results showed that expression levels of 27 mRNAs, out of 92 mRNAs, were significantly different among the four groups. Two glycolysis-related proteins, GAPDH and HK2, were increased in MPECs of DH mice compared with those in DN or CH mice. In addition, the levels of pyruvate and lactate (glycolysis end products) were significantly increased in MPECs of DH mice, but not in CH mice, compared with MPECs of CN mice. Augmentation of glycolysis by terazosin exacerbated hypoxia-induced PH in CH mice but not in DH mice. On the contrary, inhibiting GAPDH (a key enzyme of the glycolytic pathway) by koningic acid ameliorated hypoxia-induced PH in DH mice but had no effect in CH mice. These data suggest that enhanced glycolysis in diabetic mice is involved in severe hypoxia-induced PH, and glycolysis inhibition is a potential target to reduce the severe progression of PH in patients with diabetes.

NEW & NOTEWORTHY Increasing evidence shows that diabetes exacerbates the progression of pulmonary hypertension; however, its molecular mechanisms are understudied. In this study, we revealed that augmented glycolysis in diabetic pulmonary endothelial cells is involved in the development of severe PH in diabetes. Inhibition of glycolysis could be a therapeutic strategy for treating pulmonary hypertension in patients with diabetes.

diabetes complications; glucose tolerance; glycolysis; lung endothelial cell; pulmonary hypertension

INTRODUCTION

Diabetes is a global health issue characterized by hyperglycemia with profound alterations in the cardiovascular system. Major vascular complications caused by diabetes include coronary artery disease, cerebrovascular disease, peripheral arterial disease, retinopathy, and nephropathy (https://www.cdc.gov/diabetes/complications/index.html). There is growing evidence showing that diabetes also increases the risk of complications in the lung (1), such as pulmonary hypertension (PH) (2–4), chronic obstructive pulmonary disease (5), idiopathic pulmonary fibrosis (6, 7), and asthma (8).

PH is a progressive disease of pulmonary arteries and arterioles with increased pulmonary vascular resistance (PVR). The primary cause of increased PVR is a severe narrowing of vessels in the lung due to excessive proliferation of pulmonary arterial smooth muscle cells (SMCs) (9, 10) and augmented pulmonary arterial contraction (11, 12). Endothelial dysfunction also leads to PH by triggering vascular remodeling and increasing vascular tone due to

*Q. Zheng, J. T. O. Cabrera, and A. Tsuji-Hosokawa contributed equally to this work.
Correspondence: A. Makino (ay.makino@ufl.edu).
Submitted 25 September 2023 / Revised 11 October 2024 / Accepted 11 October 2024

decreased endothelium-dependent relaxation in pulmonary arteries (13–17). The persistent rise in PVR and subsequent increase in right ventricular afterload result in the right ventricle (RV) hypertrophy, right-sided heart failure, and death if untreated (18, 19). Therefore, it is critical to understand the molecular mechanisms of pulmonary endothelial dysfunction in PH.

Endothelial dysfunction is a hallmark of diabetic macro and microangiopathies (20). Thus, it is natural to anticipate that hyperglycemia-induced endothelial dysfunction is associated with the development of PH. Over the past decades, a close relationship between diabetes and PH has been established. A systematic review and meta-analytical data show that maternal diabetes increases the risk of PH in newborns (21), and comorbidity of PH is observed in patients with diabetes (22, 23). The survival rate in patients with PH with diabetes is worse than in those without diabetes (3, 24–26). An unbiased phenome-wide association study indicates that diabetes is a significant risk factor for increased pulmonary arterial pressure (PAP) and RV stress (27). We reported that diabetic patients with pulmonary arterial hypertension (PAH) exhibited aggravated right ventricular remodeling and increased RV afterload compared with nondiabetic patients with PAH (28).

The data from animal experiments also support these clinical observations. Type 1 diabetic (T1D) rats induced by high-dose streptozotocin (STZ) exhibit increases in PAP accompanied by RV remodeling (29, 30). Zucker diabetic fatty rats [a spontaneous type 2 diabetic (T2D) rat model] show increased PAP, RV hypertrophy, and media thickening in pulmonary arteries (PAs) (31). Db/db mouse (a monogenic T2D mouse model) displays decreased compliance in perfused lungs, although there is no significant change in basal PAP (20). Endothelium-dependent relaxation in PAs is attenuated due to enhanced production of NADPH oxidase-derived superoxide in T1D rats (32). In our previous study, we demonstrated that T2D mice induced by a high-fat diet with low-dose STZ or spontaneous T2D mice (KK.Cg-Ay/J, a polygenic T2D mouse model) increased the sensitivity and susceptibility to hypoxia, evidenced by higher levels of right ventricle systolic pressure (RVSP) in T2D mice than their controls after chronic hypoxia exposure (33). We now extend these observations to investigate the molecular mechanisms contributing to the increased susceptibility to chronic hypoxia-mediated PH in diabetic mice. Our data suggest that increased glycolysis in endothelial cells (ECs) contributes to exacerbating RVSP in diabetic mice exposed to hypoxia, and inhibition of glycolysis could be a potential therapeutic approach to minimize the risk of PH in patients with diabetes.

MATERIALS AND METHODS

Animal Models

Male C57BL/6NHsd mice were purchased from ENVIGO (Placentia, CA). Inducible T2D mice were generated by feeding a high-fat diet (60% kcal from fat, ENVIGO) with a single injection of low-dose STZ (75 mg/kg, ip) at the age of 6 wk (33, 34). Control and inducible T2D mice were randomly assigned into four groups: control mice in normoxia (CN), diabetic mice in normoxia (DN), control mice exposed to hypoxia (CH), and diabetic mice exposed to hypoxia (DH). At the age of 18 wk (12 wk after T2D induction), hypoxic groups were placed in a hypoxic chamber (10% O_2) for 4 wk. Male TALLYHO/Jng (TH) mice were purchased from the Jackson Laboratory and bred in our animal facility. TH mice are polygenic T2D models, and male TH mice exhibit hyperglycemia, hyperinsulinemia, dyslipidemia, and obesity (35–37). C57BL/6 mice were used as wild-type (Wt) controls according to the company's guidelines. Wt and TH mice were randomly assigned into four groups: Wt mice in normoxia (WN), TH mice in normoxia (TN), Wt mice exposed to hypoxia (WH), and TH mice exposed to hypoxia (THH). TH mice were fed with a regular laboratory diet. At the age of 6 wk, TH mice in the hypoxic group were exposed to hypoxia for 4 wk. Terazosin (TZ, 10 μg/kg, sc) (38) and koningic acid (KA, 110.4 μg/kg, sc) (39, 40) were administered using an osmotic minipump (ALZET, Cupertino, CA. Cat. No. 2004) for 4 wk. The age was matched between diabetic and control mice. Male mice were used in this study due to the difference in the onset of hyperglycemia and diabetic complications between male and female mice (41, 42). We will consider investigating the effect of sex differences on diabetes-induced severe PH in future studies.

All experimental protocols used in this study were approved by the Institutional Animal Care and Use Committee (IACUC) at The University of Arizona (UA) and the University of California, San Diego (UCSD) and conformed to the Guide for the Care and Use of Laboratory Animals published by the National Institutes of Health. The universities have been certified by the Public Health Service with Animal Welfare Assurance numbers, A3248-01 (UA) and A3033-01 (UCSD). The approved IACUC protocol numbers for this study are 14–520 (at UA) and S18185 (at UCSD). The laboratory personnel who conducted experiments took all the training required for animal handling and were certified by the IACUC. At least two investigators repeated the experiments to confirm the reproducibility. We conducted experiments in a blinded fashion wherever possible and set proper controls for every experimental plan.

Metabolic Characterization

An oral glucose tolerance test (OGTT) was performed as described previously (33, 43). After fasting the mice for 6 h, the glucose levels at the baseline were measured (0 min). The mice were then orally given glucose (2 g/kg body wt). Blood glucose levels were measured 15, 30, and 60 min after glucose administration. Lipid fractions in the plasma were measured using kits (FUJIFILM Holdings America Corp.). Plasma insulin level was measured using a kit from ALPCO Diagnostics (Salem, NH).

Assessment of RV Hemodynamic Parameters

Right ventricular systolic pressure (RVSP, a surrogate measure of pulmonary arterial systolic pressure) and Fulton index were measured to evaluate the development and progression of PH (17, 33, 44). Mice were anesthetized with 1% isoflurane mixed in 100% O_2 using an animal anesthesia system (Harvard Apparatus, Holliston, MA). A PVR-

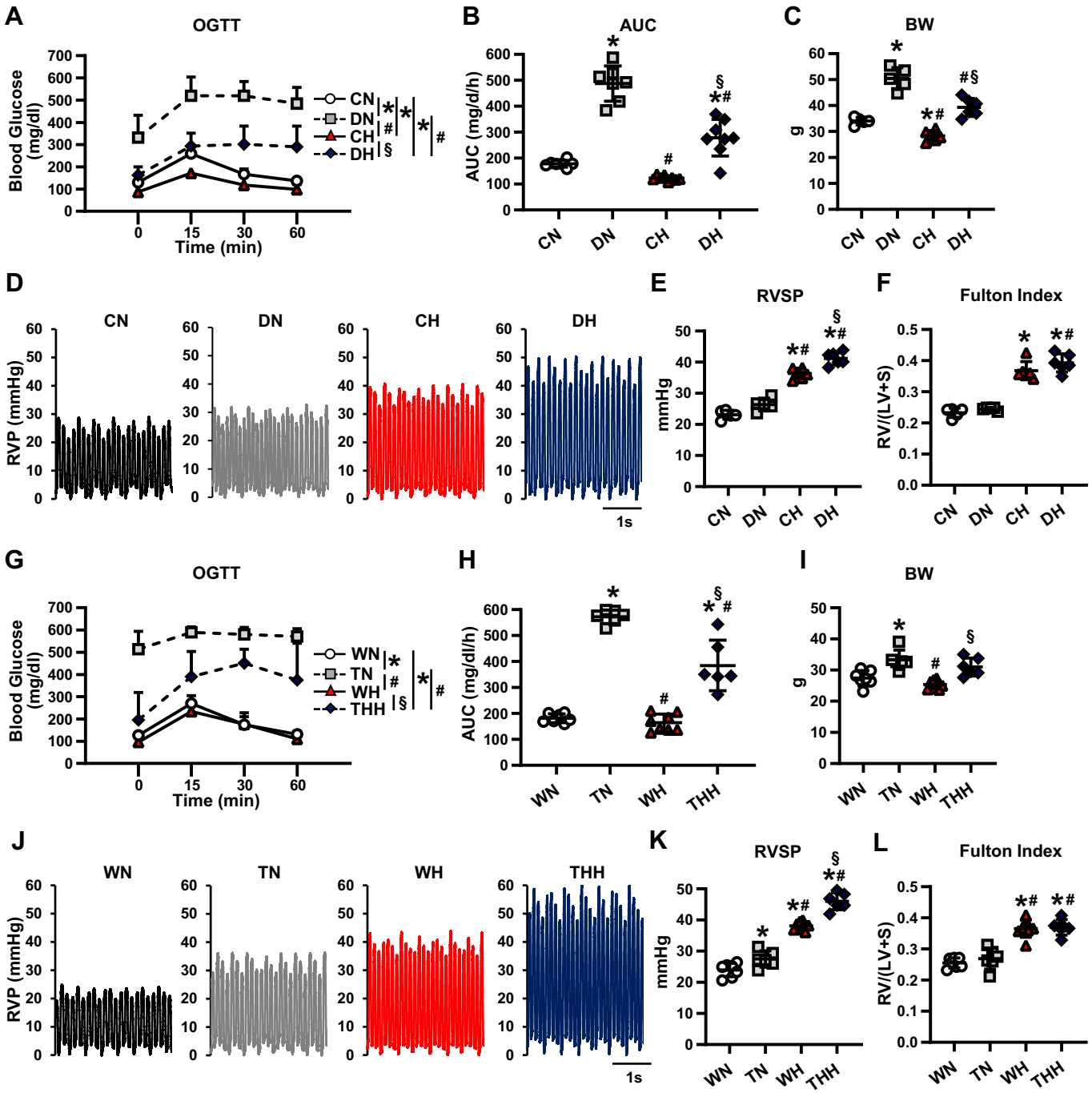

Figure 1. Chronic hyperglycemia exacerbates the development of pulmonary hypertension. Oral glucose tolerance test (OGTT, *A*) and area under the curve (AUC, *B*). Normoxia-exposed control mice (CN, $n_{mice} = 7$), normoxia-exposed diabetic mice (DN, $n_{mice} = 7$), hypoxia-exposed control mice (CH, $n_{mice} = 8$), and hypoxia-exposed diabetic mice (DH, $n_{mice} = 8$). *C*: body weight (BW). *D*: typical record of right ventricle pressure (RVP). *E*: right ventricle systolic pressure (RVSP). *F*: Fulton index. *C*, *E*–*F*: CN, $n_{mice} = 5$; DN, $n_{mice} = 5$; CH, $n_{mice} = 6$; DH, $n_{mice} = 6$. *$P < 0.05$ vs. CN, #$P < 0.05$ vs. DN, §$P < 0.05$ vs. CH. OGTT (*G*) and AUC (*H*). Normoxia-exposed wild-type mice (WN), normoxia-exposed TALLYHO/Jng mice (TN), hypoxia-exposed wild-type mice (WH), and hypoxia-exposed TALLYHO/Jng mice (THH). *I*: BW. *J*: RVP. *K*: RVSP. *L*: Fulton index. WN, $n_{mice} = 7$; TN, $n_{mice} = 6$; WH, $n_{mice} = 8$; THH, $n_{mice} = 6$. *$P < 0.05$ vs. WN, #$P < 0.05$ vs. TN, §$P < 0.05$ vs. WH. Statistical comparisons between time-response curves in *A* and *G* were made by two-way ANOVA with post hoc test (Bonferroni's multiple comparisons test). In other figures, one-way ANOVA was used for multiple comparisons, followed by Bonferroni's post hoc test, after the data passed a normality test. If the data did not pass the normality test, a nonparametric Kruskal–Wallis test was used. Data are presented as means ± SD.

1030 Millar catheter (Millar Instruments, Houston, TX) was inserted into the RV through the right external jugular vein. Hemodynamic parameters were collected via the Lab Chart software (AD Instruments, Inc., Springs, Colorado). After experiments, the RV free wall was separated from the left ventricle (LV), and Fulton index {RV/(LV + septum), a determinant of right ventricular hypertrophy due to increased afterload} was assessed.

Table 1. *Lipid profile of control and diabetic mice*

	CN (n_{mice} = 5)	DN (n_{mice} = 5)	CH (n_{mice} = 5)	DH (n_{mice} = 5)
TC, mg/dL	63.1 ± 11.0	178.6 ± 36.8*	52.2 ± 9.5#	169.3 ± 19.9*§
HDL, mg/dL	47.4 ± 8.2	90.1 ± 15.8*	40.1 ± 8.6#	94.4 ± 6.7*§
TG, mg/dL	18.6 ± 4.4	48.0 ± 28.2*	14.8 ± 1.2#	32.8 ± 7.5§
LDL/VLDL, mg/dL	12.0 ± 7.4	78.9 ± 27.6*	8.2 ± 1.3#	68.4 ± 18.9*§
Insulin, ng/mL	0.75 ± 0.04	1.63 ± 0.65*	0.72 ± 0.03#	0.83 ± 0.04#

Data are presented as means ± SD. *n* shows the number of mice. CH, hypoxia-exposed control mouse; CN, normoxia-exposed control mouse; DH, hypoxia-exposed diabetic mouse; DN, normoxia-exposed diabetic mouse; HDL, plasma high-density lipoprotein; LDL, plasma low-density lipoprotein; TC, plasma total cholesterol; TG, plasma triglyceride; VLDL, plasma very low-density lipoprotein. *P < 0.05 vs. CN. #P < 0.05 vs. DN. §P < 0.05 vs. CH. After the data passed a normality test, one-way ANOVA was used for multiple comparisons, followed by Bonferroni post hoc test. If the data did not pass the normality test, a nonparametric test (Kruskal–Wallis) was used.

Mouse Pulmonary Endothelial Cell Isolation

Mouse pulmonary endothelial cells (MPECs) were isolated, as previously described (17, 33). Dissected mouse lung tissues were digested with M199 containing 2 mg/mL collagenase I and 0.6 U/mL dispase II. The cell suspension was incubated with CD31-coated Dynal magnetic beads (Thermo Fisher Scientific) for 1 h at 4°C. ECs attached to the beads were captured by a Dynal magnet (Thermo Fisher Scientific). The purity of cells is >90%.

qPCR

MPECs were freshly isolated from mice and stored at −80°C before the next step. RNA was isolated from MPECs using miRNeasy kit (QIAGEN, Chatsworth, CA), and cDNA was synthesized using RT2 First Strand Kit (QIAGEN). To assess multiple gene levels, we made a custom qPCR plate (RT^2-Profiler PCR Arrays, QIAGEN) using 92 selected genes. The 384-well plate consists of quadruple 96 genes, and 96 genes include 92 selected genes plus four genes for loading and plate controls (Supplemental Table S1). The genes critical for endothelial functions were chosen based on the following criteria: *a*) endothelium-derived relaxing and contracting factors and their regulators; *b*) modifiers of cytosolic, mitochondrial, and endoplasmic reticulum calcium concentrations; and *c*) regulators of EC proliferation/migration/apoptosis. qPCR was conducted according to the manufacturer's instructions. The efficiency correlated ΔCt method was used to determine the level, in arbitrary units, of each mRNA relative to *Actb*. Any exclusion decision was supported by Grubbs' test. One-way ANOVA was used for multiple comparisons, followed by Bonferroni's multiple comparisons test as a post hoc test.

Western Blot Analysis

Freshly isolated MPECs were lysed, and proteins were separated using SDS-PAGE. The primary antibody information is listed in Supplemental Table S2. The expression levels of the proteins were normalized to the corresponding Actin signal.

Pyruvate and Lactate Assay

Pyruvate and lactate levels were determined using a Fluorometric Assay Kit from Biovision (Cat. No. K609, and K607, Milpitas, CA). MPECs were homogenized, and supernatant was collected for the study. The protein concentration was measured using Bradford Assay and adjusted among the samples. The fluorescence intensity (Ex/Em = 535/587 nm) was measured using a fluorescent plate reader.

Statistical Analysis

We conducted data analysis in a blinded fashion wherever possible and set proper controls for every experimental plan. The mouse number and independent experiment number are described in the figure legends. Statistical analysis was performed using GraphPad Prism 9.1 (La Jolla, CA). After the data passed a normality test, the two-tailed Student's *t* test was used to compare two groups, and one-way ANOVA was used for multiple comparisons, followed by Bonferroni post hoc test. If the data did not pass the normality test, a nonparametric test (Mann–Whitney for two groups, Kruskal–Wallis for multiple comparisons) was used. Statistical comparisons between time-response curves were made using two-way ANOVA with Bonferroni post hoc test. Differences were considered to be statistically significant when $P < 0.05$. Data are presented as mean ± SD.

RESULTS

Diabetes Exacerbates Hypoxia-Induced PH

We first investigated how diabetic mice respond to chronic hypoxia. Our inducible T2D mice exhibited hyperglycemia, abnormal glucose tolerance, increased body weight, hyperinsulinemia, and dyslipidemia (Fig. 1, *A–C*, and Table 1); this model is close to human type 2 diabetes induced by Western diet (34, 43). Four-week hypoxic exposure partially improved glucose tolerance and significantly decreased body weight in both control (CH) and T2D (DH) mice compared with normoxia-exposed mice (CN and DN); however, the degree of glucose tolerance was still worse in DH mice than in CN and CH mice (Fig. 1, *A* and *B*). Hypoxia did not affect the level of lipid fractions in control and diabetic mice, while DH mice showed a significant decrease in insulin levels compared with DN mice (Table 1). Importantly, DH mice developed more severe PH than the CH mice, evidenced by the significant increase in RVSP in DH mice compared with CH mice (Fig. 1*E*). Fulton index was higher in CH compared with CN, and there was no statistical difference in Fulton index between CH and DH (Fig. 1*F*).

To confirm the effects of hyperglycemia on PH development, we used TH mice (a spontaneous T2D mouse model) to repeat the experiment. Normoxia-exposed TH mice (TN) displayed abnormal glucose tolerance accompanied by increased body weight (Fig. 1, *G*, *H* and *I*). In line with the data of inducible T2D mice, glucose tolerance was markedly improved in hypoxia-exposed TH mice (THH) than TN mice

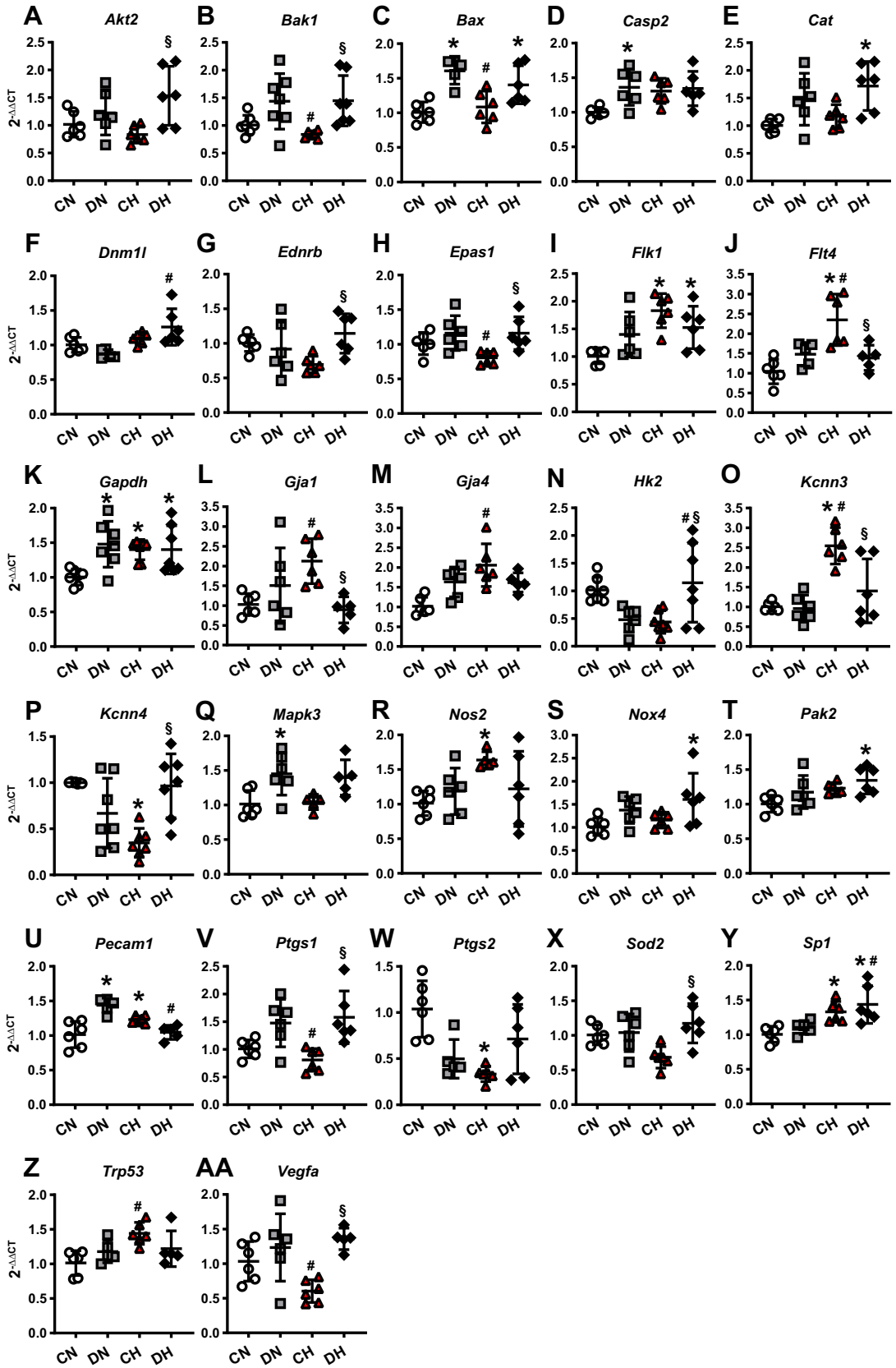

but still worse in THH than wild-type mice exposed to normoxia (WN) and hypoxia (WH) (Fig. 1*G*). Mice exposed to chronic hypoxia (WH and THH) significantly increased RVSP and Fulton index. Notably, the hypoxia-induced increase in RVSP was significantly greater in THH than in WH mice (Fig. 1*K*), whereas Fulton index was not significantly changed in THH compared with WH (Fig. 1*L*). These results suggest that chronic hyperglycemia makes mice prone to hypoxia-induced PH.

Identification of Genes Altered by Hypoxia and Diabetes

We previously demonstrated that pulmonary endothelial dysfunction is associated with the development of hypoxia-induced PH (17, 33). To define the molecular mechanisms by which diabetes accelerates endothelial damage in hypoxia-induced PH mice, we conducted semi-unbiased gene screening experiments. Ninety-two genes were selected based on their critical roles in endothelial functions (Supplemental Table S1). We compared mRNA levels of these genes in MPECs isolated from CN, CH, DN, and DH mice using real-time PCR. Among the 92 genes, 27 genes showed statistical significance among the four groups (Fig. 2). The significant genes are related to *1*) cell apoptosis (*Bak1*, *Bax*, *Casp2*, *Dnm1l*, *Epas1*, *Gapdh*, *Hk2*, *Mapk3*, *Sp1*, and *Trp53*), *2*) glycolysis (*Gapdh* and *Hk2*), *3*) endothelium-dependent relaxations (*Atp2a3*, *Cat*, *Ednrb*, *Gja1*, *Gja4*, *Kcnn3*, *Kcnn4*, *Nos2*, *Nox4*, *Ptgs1*, *Ptgs2*, and *Sod2*), *4*) handling of cytosolic [Ca^{2+}], mitochondrial [Ca^{2+}], and endoplasmic reticulum [Ca^{2+}] (*Atp2a3* and *Hk2*), and *5*) angiogenesis (*Akt2*, *Flk1*, *Flt4*, *Mapk3*, *Pak2*, *Pecam1*, and *Vegfa*). *Flt1*, *Flk4*, *Gapdh*, *Kcnn3*, *Nos2*, *Pecam1*, and *Sp1* levels were significantly upregulated in CH mice compared with CN mice. Increased *Flt4* and *Kcnn3* levels in CH mice were significantly decreased in DH mice. On the other hand, *Kcnn4* and *Ptgs2* mRNA levels were reduced in CH mice compared with CN mice, and Kcnn4 was dramatically increased in DH mice compared with CH mice. Based on the comparison between CH and DH mice, the expression levels of *Akt2*, *Bak1*, *Ednrb*, *Epas1*, *Hk2*, *Kcnn4*, *Ptsg1*, *Sod2*, and *Vegfa* were significantly higher in DH mice than in CH mice, and *Flt4*, *Gja1,* and *Kcnn3* levels were lower in DH mice than CH mice. As we saw significant differences in apoptosis- and glycolysis-related genes in DH mice (compared with CH mice), we next conducted experiments to confirm protein levels of the genes related to apoptosis and glycolysis.

Hypoxia and Hyperglycemia Regulate Expression Levels of Glycolysis-Related Proteins, but Not Apoptosis-Related Proteins in MPECs

Bak1, Bax, and Bcl-xL regulate mitochondria-mediated apoptosis; Bak1 and Bax are proapoptotic proteins, and Bcl-xL acts as an antiapoptotic protein. Although Bak1 mRNA level was altered by hypoxia and hyperglycemia, there was no significant difference in protein expression levels of Bak1 among the four groups (i.e., CN, CH, DN, and CH mice) (Fig. 3*A*). The ratio of Bax/Bcl-xL is commonly used to characterize apoptosis in cells. Hypoxia exposure significantly decreased Bax/Bcl-xL ratio in CH mice because of an extensive increase in Bcl-xL (Fig. 3, *B–D*). CASP2 and p53 are also pro-apoptotic proteins; however, there was no significant difference among the four groups (Supplemental Fig. S1). It is well known that hypoxia increases GAPDH, and we also observed a significant increase in GAPDH in CH and DH mice compared with CN and DN (Fig. 3*E*). The protein level of HK2 was significantly decreased in DN and CH mice compared with CN mice. In contrast, HK2 level was significantly increased in DH mice compared with DN and CH mice (Fig. 3*F*). These data suggest that the activated signaling pathway related to glycolysis is involved in the development of severe PH in diabetic mice.

Pyruvate and Lactate Levels Are Increased in MPECs Isolated from Hypoxia-Exposed T2D Mice

As GAPDH and HK2 levels are significantly increased in MPECs in DH mice, we expect that glycolysis might be augmented in MPECs from DH mice. Enhanced glycolysis increases pyruvate production and lactate accumulation in the cells (45); therefore, we measured pyruvate and lactate levels in MPECs isolated from CN, DN, CH, and DH mice. The pyruvate level was significantly higher in DH mice than in CN and CH mice (Fig. 4*A*). The lactate level was also increased in DH mice (Fig. 4*B*), suggesting that glycolysis is enhanced in pulmonary ECs in DH mice.

Stimulation of Glycolysis with Terazosin Further Increases RVSP in Hypoxia-Exposed Control Mice, but Not in Hypoxia-Exposed Diabetic Mice

Next, we examined whether excess glycolysis would affect hypoxia-induced PH. Terazosin (TZ) is a Food and Drug Administration-approved α_1-adrenoceptor blocking agent used to treat high blood pressure and prostatic hyperplasia. It is also known to activate phosphoglycerate kinase 1 (PGK1); therefore, it stimulates glycolysis (38). TZ (10 μg/kg) or saline (vehicle) was administered to mice for 4 wk using an osmotic minipump. At the end point, we conducted OGTT to evaluate the effect of TZ on the diabetic status and RVSP for the development of hypoxia-induced PH. TZ administration did not alter glucose tolerance (Fig. 5, *A* and *B*) and body weight (Fig. 5*C*) in hypoxia-exposed control mice (CH-TZ) and diabetic mice (DH-TZ) compared with vehicle-administered hypoxia-exposed control (CH) and diabetic (DH) mice. TZ administration significantly increased RVSP in CH mice (comparison between CH and CH-TZ, Fig. 5*F*). In contrast, TZ administration did not affect RVSP in DH mice (comparison between DH and DH-TZ, Fig. 5*G*), suggesting that the enhanced glycolysis seen in diabetic mice might be the independent risk factor of hypoxia-

Figure 2. Genes with altered mRNA levels by chronic hypoxia and hyperglycemia treatment. mRNA was isolated from mouse pulmonary endothelial cells (MPECs), and real-time PCR was used to determine mRNA levels. *A*: *Akt2*. *B*: *Bak1*. *C*: *Bax*. *D*: *Casp2*. *E*: *Cat*. *F*: *Dnm1l*. *G*: *Ednrb*. *H*: *Epas1*. *I*: *Flk1*. *J*: *Flt4*. *K*: *Gapdh*. *L*: *Gja1*. *M*: *Gja4*. *N*: *Hk2*. *O*: *Kcnn3*. *P*: *Kcnn4*. *Q*: *Mapk3*. *R*: *Nos2*. *S*: *Nox4*. *T*: *Pak2*. *U*: *Pecam1*. *V*: *Ptgs1*. *W*: *Ptgs2*. *X*: *Sod2*. *Y*: *Sp1*. *Z*: *Trp53*. *AA*: *Vegfa*. $n_{mice} > 5$ per group. *$P < 0.05$ vs. CN, #$P < 0.05$ vs. DN, §$P < 0.05$ vs. CH. Any exclusion decision was supported by Grubbs' test. One-way ANOVA was used for multiple comparisons, followed by Bonferroni's multiple comparisons test as a post hoc test. The genes presented here are statistically significant among the four groups with one-way ANOVA ($P < 0.05$). The significance shown in each figure is the result of Bonferroni's multiple comparisons test as a post hoc test. Data are presented as means ± SD.

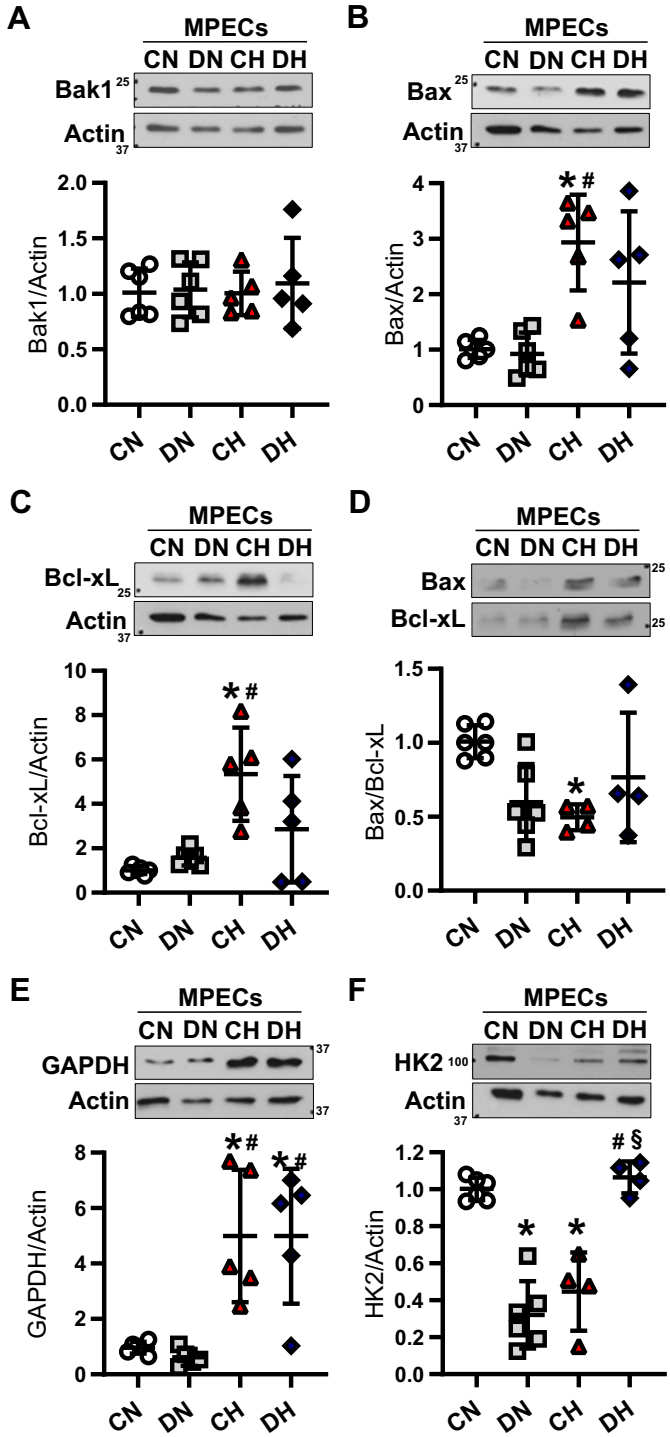

Figure 3. Chronic hypoxia and hyperglycemia differentially affect the protein expression of HK2 and GAPDH. The protein levels of apoptosis- and glycolysis-related genes are compared among four groups. Protein samples were isolated from MPECs. *A*: Bak1. *B*: Bax. *C*: Bcl-xL. *D*: Bax/Bcl-xL. *E*: GAPDH. *F*: HK2. $n_{mice} > 4$ per group. *$P < 0.05$ vs. CN, #$P < 0.05$ vs. DN, §$P < 0.05$ vs. CH. After the data passed a normality test, one-way ANOVA was used for multiple comparisons, followed by Bonferroni post hoc test. If the data did not pass the normality test, a nonparametric test (Kruskal–Wallis) was used. Data are presented as means ± SD. MPECs, mouse pulmonary endothelial cells.

induced PH. Fulton index was slightly, but significantly, increased in DH-TZ mice compared with DH mice.

Inhibition of Glycolysis via Koningic Acid Administration Prevents Aggravated Hypoxia-Induced PH in Diabetic Mice

To test our hypothesis that excess glycolysis in diabetic mice exacerbates hypoxia-induced PH, we inhibited glycolysis using koningic acid (KA, a GAPDH inhibitor). We administered KA in mice using an osmotic minipump at 110.4 μg/kg (sc) (39, 40) for 4 wk. KA administration did not affect the diabetic status and body weight, evidenced by no difference in OGTT and body weight between DH and KA-administered DH mice (DH-KA) (Fig. 6, *A–C*). However, DH-KA mice exhibited a significant decrease in RVSP compared with DH mice, and the level of RVSP was close to CH mice (Fig. 6, *E* and *G*). There was no significant difference in Fulton index between DH and DH-KA mice (Fig. 6*H*). KA did not affect RVSP and Fulton index in CH mice (Fig. 6, *F* and *H*). We also measured pyruvate concentration in MPECs and found that MPECs from DH-KA mice showed a significant decrease in pyruvate levels compared with MPECs from DH mice (Fig. 6*I*). These data suggest that increased glycolysis in diabetic mice is one of the causes of severe hypoxia-induced PH in diabetic mice.

DISCUSSION

Other investigators and we reported that preconditioning of diabetes worsens the progress of PH in patients (3, 21, 22, 26, 28, 46) and PH animal models (20, 29, 31–33). The World Health Organization classifies pulmonary hypertension into five different types: Group 1: pulmonary arterial hypertension; Group 2: pulmonary hypertension due to left heart disease; Group 3: pulmonary hypertension due to lung disease; Group 4: pulmonary hypertension due to chronic blood clots in the lungs; and Group 5: pulmonary hypertension due to unknown causes. There are more reports showing the effect of diabetes preconditioning on

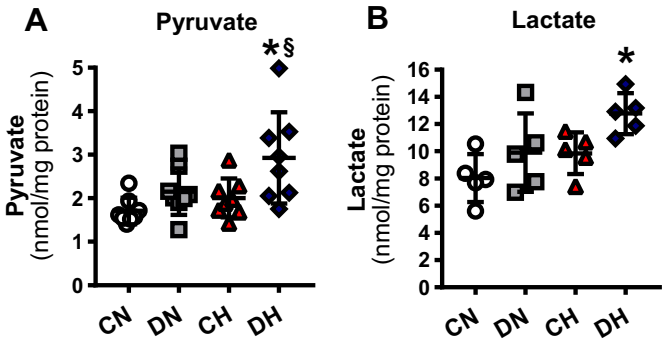

Figure 4. Pyruvate and lactate levels are increased in MPECs isolated from DH mice. *A*: pyruvate levels in MPECs isolated from CN, CH, DN, and DH mice. $n_{mice} = 8$ per group. *B*: lactate levels in MPECs isolated from CN, CH, DN, and DH mice. $n_{mice} = 5$ per group. *$P < 0.05$ vs. CN and §$P < 0.05$ vs. CH. One-way ANOVA was used for multiple comparisons, followed by Bonferroni post hoc test. Data are presented as means ± SD. CH, hypoxia-exposed control mouse; CN, normoxia-exposed control mouse; DH, hypoxia-exposed diabetic mouse; DN, normoxia-exposed diabetic mouse; MPECs, mouse pulmonary endothelial cells.

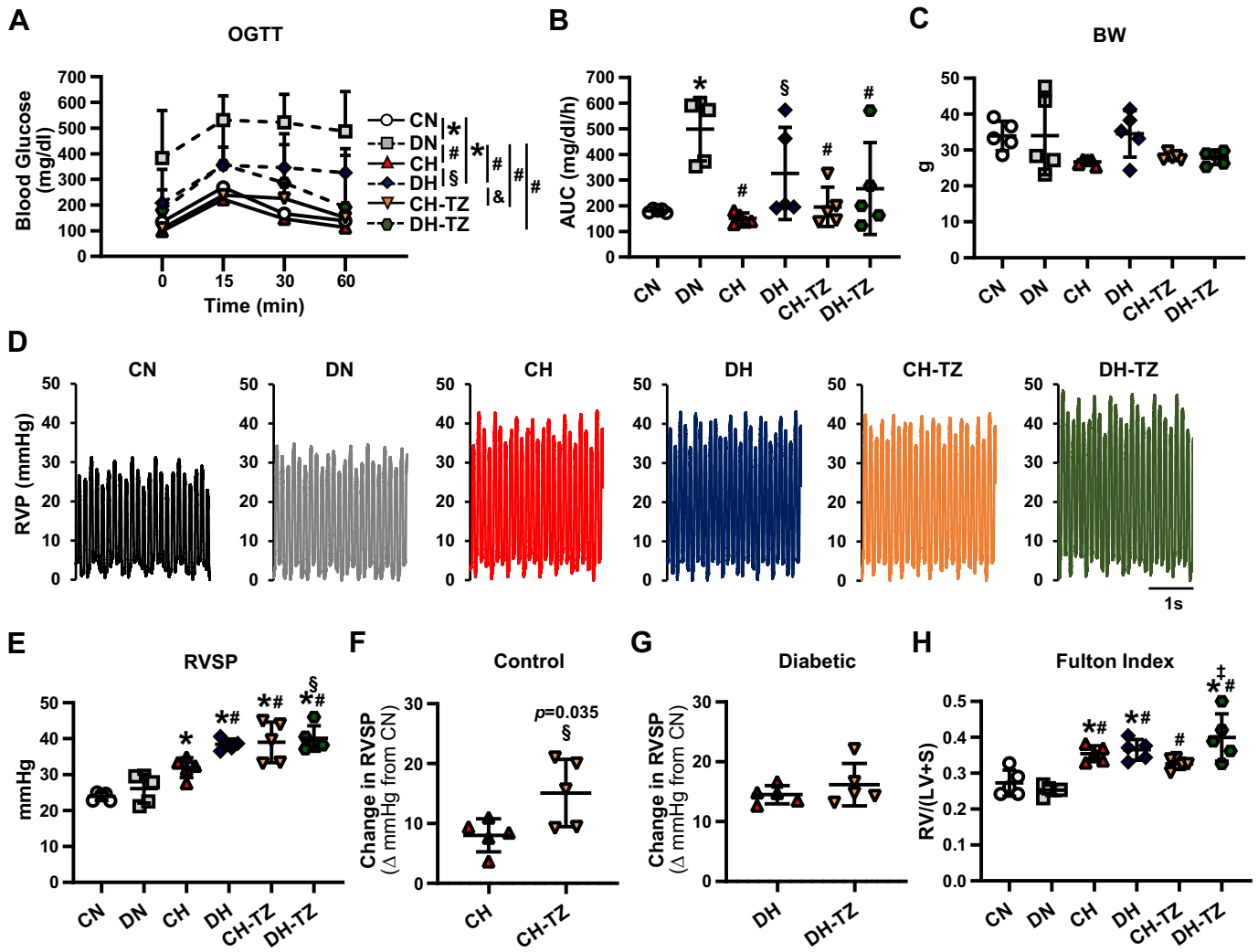

Figure 5. Stimulating glycolysis by terazosin exacerbates hypoxia-induced PH in control mice but not in diabetic mice. *A*: OGTT. Hypoxia-exposed terazosin (TZ)-treated control mice, CH-TZ; hypoxia-exposed TZ-treated diabetic mice, DH-TZ. *B*: AUC. *C*: BW. *D*: RVP. *E*: RVSP. *F*: change of RVSP by TZ treatment in CH mice (ΔmmHg from CN). *G*: change of RVSP by TZ treatment in DH mice (ΔmmHg from CN). *H*: Fulton index. $n_{mice} = 5$ per group. *$P <$ 0.05 vs. CN, #$P < 0.05$ vs. DN, §$P < 0.05$ vs. CH, &$P < 0.05$ vs. DH, and ‡$P < 0.05$ vs. CH-TZ. Statistical comparison between time-response curves in A was made by two-way ANOVA with Bonferroni post hoc test. In B, *C*, *E*, and *H*, one-way ANOVA followed by Bonferroni post hoc test was performed. In *F* and *G*, two-tailed Student's *t* test was used to compare two groups. Data are presented as means ± SD. AUC, area under the curve; CH, hypoxia-exposed control mouse; CN, normoxia-exposed control mouse; DH, hypoxia-exposed diabetic mouse; DN, normoxia-exposed diabetic mouse; RVP, right ventricle pressure; RVSP, right ventricle systolic pressure.

the prevalence and progression of PH in Group 1 patients (22, 26, 28, 46, 47); however, patients in other PH classes are also susceptive to diabetes (3, 4, 21). In this study, we investigated the molecular mechanisms by which diabetes exacerbates hypoxia-induced PH (Group 3 PH mouse model) using diabetic mice. The main findings of our study are: *1*) diabetic mice exhibit a greater increase in RVSP after hypoxia exposure compared with control mice, *2*) glycolysis-related genes are dysregulated in MPECs from hypoxia-exposed diabetic mice, and *3*) inhibition of GAPDH (a key enzyme of the glycolytic pathway) in diabetic mice prevents exacerbated increase in RVSP after hypoxia exposure.

Inducible T2D mice and spontaneous T2D mice (TH mice) display increased sensitivity or susceptibility to hypoxia-induced PH (Fig. 1). This result aligns with our previous report using genetically modified T2D mice (KK. Cg-Ay/J mice) (33). Although RVSP was significantly increased in hypoxia-exposed diabetic (DH) mice compared with hypoxia-exposed control (CH) mice, Fulton index was not altered by diabetic preconditioning. The possible reason for further increase in RVSP or more severe hypoxia-induced PH in diabetic mice without changing Fulton index would be *1*) RV hypertrophy was maximally developed by hypoxia exposure; therefore, further increase in RVSP seen in diabetic mice could not alter Fulton index, *2*) the change of Fulton index would take more time after elevated RVSP in diabetic mice, and *3*) the RV underwent decompensated hypertrophy or dilated RV cardiomyopathy in diabetic mice with hypoxia-induced PH. This is a unique phenomenon requiring further experiments to identify the relation between RVSP and Fulton index in diabetes.

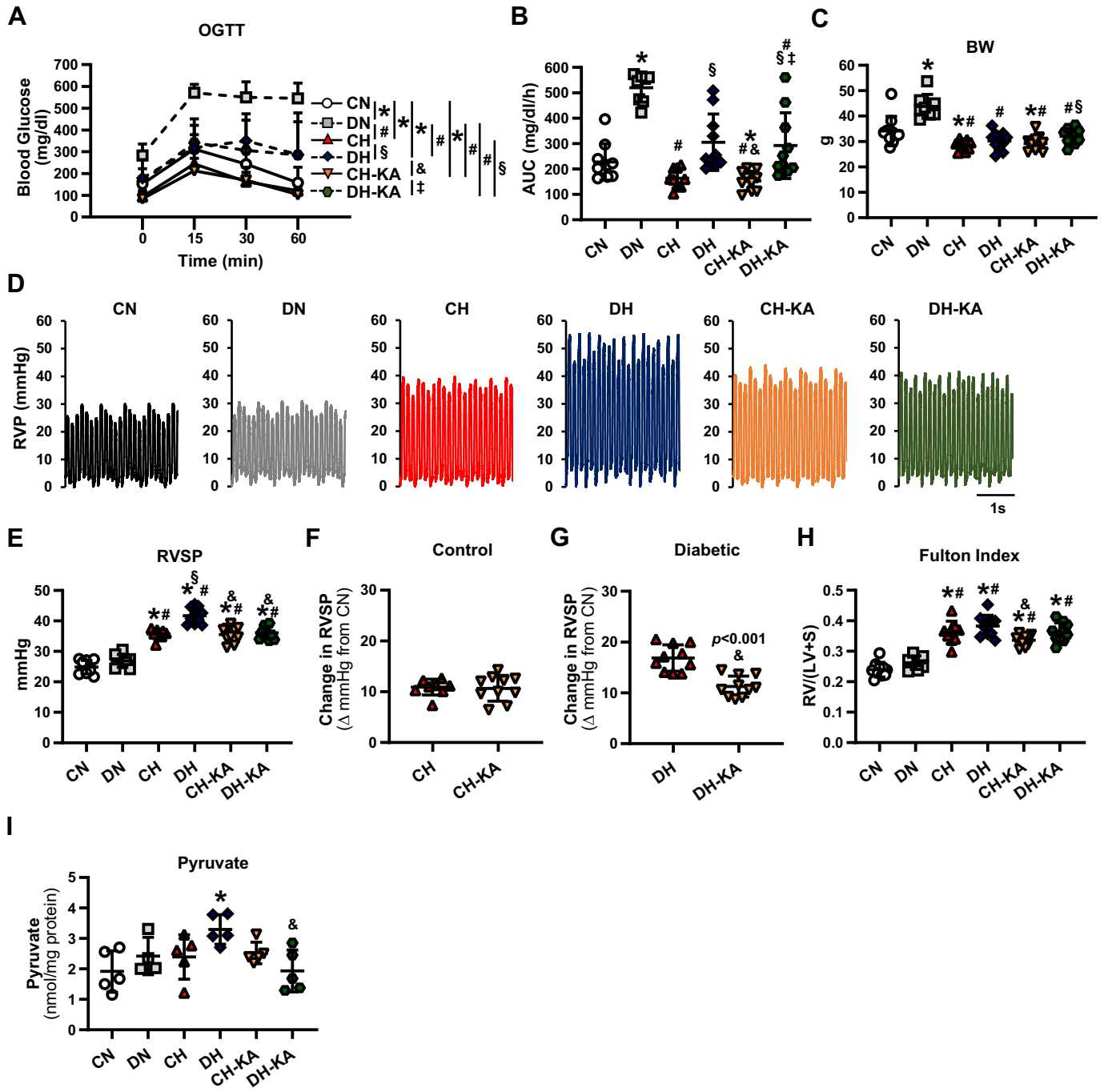

Figure 6. Chronic administration of GAPDH inhibition by koningic acid decreases RVSP in DH mice but not in CH mice. OGTT (*A*) and AUC (*B*). Hypoxia-exposed koningic acid (KA)-treated control mice, CH-KA; hypoxia-exposed KA-treated diabetic mice, DH-KA. *C*: BW. *D*: RVP. *E*: RVSP. *F*: change of RVSP by KA treatment in CH mice (ΔmmHg from CN). *G*: change of RVSP by KA treatment in DH mice (ΔmmHg from CN). *H*: Fulton index. *A*, *B*, *D*–*F*; CN, $n_{mice} = 10$; DN, $n_{mice} = 8$; CH, $n_{mice} = 9$; DH, $n_{mice} = 10$; CH-KA, $n_{mice} = 10$; DH-KA, $n_{mice} = 10$. *I*: pyruvate concentration in MPECs. CN, $n_{mice} = 5$; DN, $n_{mice} = 4$; CH, $n_{mice} = 5$; DH, $n_{mice} = 5$; CH-KA, $n_{mice} = 5$; DH-KA, $n_{mice} = 5$. *$P < 0.05$ vs. CN, #$P < 0.05$ vs. DN, §$P < 0.05$ vs. CH, &$P < 0.05$ vs. DH, and ‡$P < 0.05$ vs. CH-KA. Statistical comparison between time-response curves in A was made by two-way ANOVA with Bonferroni post hoc test. In *B*, *E*, *H*, and *I*, one-way ANOVA followed by Bonferroni post hoc test was performed. For *C*, a nonparametric Kruskal–Wallis test with Dunn's post hoc test was used. In *F* and *G*, two-tailed Student's *t* test was used to compare two groups. Data are presented as means ± SD. AUC, area under the curve; CH, hypoxia-exposed control mouse; CN, normoxia-exposed control mouse; DH, hypoxia-exposed diabetic mouse; DN, normoxia-exposed diabetic mouse; RVP, right ventricle pressure; RVSP, right ventricle systolic pressure.

We have reported that endothelial function was attenuated in DH mice compared with CH mice (33); therefore, we aimed to identify the genes altered in DH mice compared with CH mice in this study. Among 27 genes altered by hypoxia and/or hyperglycemia, we selected four genes involved in cell apoptosis (*Bak1*, *Bax*, *Casp2*, and *Trp53*) and two genes related to glycolysis (*Gapdh* and *Hk2*) for further validation of their protein expression levels. Bax/Bcl-xl ratio

in MPECs was significantly decreased in CH mice compared with CN mice (Fig. 3), whereas Casp2 and p53 levels were not changed (Supplemental Fig. S1). These data suggest that hypoxia makes endothelial cells more resistant, or adaptive, to apoptosis. It is well characterized that smooth muscle cells from PH animal models and patients with PH are proliferative and apoptosis resistant. However, the expression levels of pro- and antiapoptotic peptides in the lung or pulmonary ECs during PH are still controversial in the literature. We have previously reported that Bax/Bcl-xl ratio and/or p53 levels are increased in the lungs of mice with hypoxia-induced PH (48) and rats with Sugen/hypoxia-induced severe PH (49). Wakasugi et al. (50), however, showed a significant decrease in p53 protein levels in the lungs of mice with hypoxia-induced PH. We do not have a good explanation for the difference between current and previous studies; one of the potential reasons for the different results is that the gene expression levels obtained from the lung samples could be influenced by other cell types, including an unignorable number of epithelial cells. Therefore, identifying mRNA/protein levels in isolated pulmonary ECs would give us more accurate assessments of endothelial-specific alteration induced by hypoxia. The timing of sampling is also critical. Breault et al. (51) indicated that endothelial apoptosis is enhanced at the early stage of PH, while ECs become more apoptosis-resistant at the late stage of PH.

There is increasing evidence showing that abnormal glycolysis is involved in the development of PH (52). ^{18}FDG uptake is a useful indicator of tissue glycolysis, and it has been reported that ^{18}FDG uptake in the lung is significantly increased in patients with idiopathic PAH and rats with monocrotaline-induced PH (53). Pulmonary arterial remodeling is an important pathological feature in patients with PAH and animals with severe experimental PH, and enhanced proliferation and metabolic shift from oxidative phosphorylation to glycolysis in pulmonary arterial smooth muscle cells (PASMCs) are indicated as important causes for pulmonary vascular remodeling in PAH/PH (54, 55). Pyruvate, a final product of glycolysis, is catalyzed by pyruvate dehydrogenase (PDH) into acetyl-CoA that drives oxidative phosphorylation in the mitochondria. Pyruvate dehydrogenase kinase (PDK) is a kinase enzyme that inactivates PDH. It has been reported that the expression of PDK is significantly increased in PASMCs isolated from patients with idiopathic PAH and animals with experimental PH. Inhibition of PDK by dichloroacetate significantly attenuates PASMC proliferation and ameliorates experimental PH in animal models (55, 56); whether dichloroacetate is indeed effective in treating PAH in patients is currently undergoing clinical trial. Altered glycolytic protein expression and/or activity is reported in pulmonary ECs, fibroblasts, and inflammatory cells in patients with PAH and animals with experimental PH (57–61). Xu et al. (57) reported a significant increase in glycolytic rate in pulmonary arterial ECs from patients with idiopathic PAH, and this phenomenon has been observed by other investigators as well (58, 59). Increased lactate formation is observed in fibroblasts isolated from hypoxia-exposed bovine and patients with PAH (60) and macrophages isolated from Sugen/hypoxia-induced PH rats and hypoxia-induced PH mice.

Glucose is first catalyzed by hexokinases in the glycolysis pathway. Hexokinases have five isoforms and pulmonary ECs predominantly express HK1 and HK2. Hyperglycemia decreased HK2 protein expression (Fig. 3) due partly to the compensatory mechanism of excess glucose level (62, 63). HK2 level was also reduced by hypoxia (Fig. 3 and Supplemental Table S3); however, HK1 levels remained high (Supplemental Fig. S2 and Supplemental Table S3), resulting in no significant change in endothelial glycolysis in hypoxia-exposed control mice (Fig. 4).

GAPDH is a critical enzyme in glycolysis, which catalyzes glyceraldehyde-3-phosphate to glycerate-1,3-bisphosphate. KA is a selective GAPDH inhibitor via its binding to the Cys149 residue in the catalytic site of GAPDH (64). We found that inhibition of GAPDH by KA significantly decreased RVSP in hypoxia-exposed T2D mice, but not in hypoxia-exposed control mice, suggesting that diabetes precondition makes mice more prone to hypoxia-induced PH via augmenting endothelial cell glycolysis. In our study, glycolysis inhibition by KA did not affect RVSP levels in control mice after hypoxia exposure (Fig. 6). Hypoxia exposure in control mice also showed no difference in pyruvate and lactate production in MPECs compared with those in normoxia-exposed control mice (Fig. 4). These data suggest that endothelial glycolysis might not contribute to the development of hypoxia-induced PH in control mice. On the contrary, Cao et al. (58) reported that hypoxia exposure increased endothelial glycolysis via increasing *Pfkfb3* in pulmonary ECs; therefore, inhibition of *Pfkfb3* in ECs partially reduced RVSP in hypoxia-exposed control mice. Based on RNAseq data previously conducted in our laboratory (17), the mRNA level of *Pfkfb*, including *Pfkfb3*, in MPECs from hypoxia-exposed mice was not significantly different from MPECs from normoxia-exposed mice (Supplemental Table S3). Further study is required to explain the difference of *Pfkfb* expression pattern in different studies.

The TZ data support our hypothesis that increased glycolysis by hyperglycemia (i.e., DH mice) further exacerbates PH in CH mice (Fig. 5). We used TZ as a glycolysis enhancer in this study; however, TZ is commonly used as an α_1 adrenergic receptor antagonist and reduces systemic pressure. If TZ affects pulmonary vascular resistance as an α_1 adrenergic receptor antagonist rather than a glycolysis enhancer, we should see a decrease in RVSP but not the increase in RVSP we observed in CH mice. Therefore, the effect of TZ as an α_1 adrenergic receptor on pulmonary circulation might be masked by increased pulmonary resistance caused by enhanced endothelial glycolysis. The detailed mechanisms, however, require additional experiments.

The limitation of this study is that we administered the inhibitors systematically, which affects many cell types, including SMCs. SMC remodeling and increased contraction are the cause of hypoxia-induced PH in control mice; however, we previously reported that the increased RVSP in hypoxia-exposed diabetic (DH) mice compared with hypoxia-exposed control (CH) mice is not caused by SMC dysfunction, but via endothelial dysfunction (33). Isolated MPECs from DH showed increased glycolysis compared with CH (Fig. 4), and KA administration in DH mice decreased endothelial glycolysis (Fig. 6). Therefore, the improvement of hypoxia-induced PH via KA administration in diabetic mice might be due to reduced endothelial

glycolysis. However, there is still a possibility that KA altered SMC functions in DH and reduced RVSP. KA is a selective inhibitor of GAPDH, a key enzyme in a glycolytic pathway. KA administration decreased pyruvate formation in MPECs and reduced RVSP in DH mice; therefore, we concluded that glycolysis is involved in the severe PH in diabetic mice. However, some might think the live measurement of glycolysis is required instead of the byproduct of glycolysis (i.e., pyruvate). In the current setting, we encountered the difficulty of assessing glycolysis in cultured MPECs after bead isolation from hypoxia-exposed mice. Methodological development is required in future studies.

In the present study, glycolysis inhibition by KA markedly suppressed hypoxia-induced PH in T2D mice. These promising preclinical findings, along with glycolytic changes in ECs, provide a strong rationale for the clinical testing of GAPDH inhibitors in treating PH, which may shed new light on the treatment for severe PH in diabetes.

DATA AVAILABILITY

All data in the current study are available from the corresponding author upon reasonable request.

SUPPLEMENTAL MATERIAL

Supplemental Tables S1–S3 and Supplemental Figs. S1 and S2: https://doi.org/10.6084/m9.figshare.26382538.

ACKNOWLEDGMENTS

The graphical abstract was created with permission from BioRender.com.

GRANTS

This work was supported by grants from the National Heart, Lung, and Blood Institute of the National Institutes of Health (HL146764, HL154754, and HL142214) and the Department of Defense (W81XWH2110472).

DISCLOSURES

No conflicts of interest, financial or otherwise, are declared by the authors.

AUTHOR CONTRIBUTIONS

A.M. conceived and designed research; Q.Z., J.T.O.C., A.T.-H., and F.J.R. performed experiments; Q.Z., J.T.O.C., A.T.-H., F.J.R., and A.M. analyzed data; Q.Z., J.T.O.C., A.T.-H., H.C., J.X.-J.Y., J.W., and A.M. interpreted results of experiments; Q.Z., J.T.O.C., A.T.-H., and A.M. prepared figures; Q.Z. and A.M. drafted manuscript; F.J.R., H.C., J.X.-J.Y., J.W., and A.M. edited and revised manuscript; Q.Z., J.T.O.C., A.T.-H., F.J.R., H.C., J.X.-J.Y., J.W., and A.M. approved final version of manuscript.

REFERENCES

1. **Ehrlich SF**, **Quesenberry CP Jr**, **Van Den Eeden SK**, **Shan J**, **Ferrara A.** Patients diagnosed with diabetes are at increased risk for asthma, chronic obstructive pulmonary disease, pulmonary fibrosis, and pneumonia but not lung cancer. *Diabetes Care* 33: 55–60, 2010. doi:10.2337/dc09-0880.
2. **Lang IM**, **Simonneau G**, **Pepke-Zaba JW**, **Mayer E**, **Ambroz D**, **Blanco I**, **Torbicki A**, **Mellemkjaer S**, **Yaici A**, **Delcroix M.** Factors associated with diagnosis and operability of chronic thromboembolic pulmonary hypertension. A case-control study. *Thromb Haemost* 110: 83–91, 2013. doi:10.1160/TH13-02-0097.
3. **Abernethy AD**, **Stackhouse K**, **Hart S**, **Devendra G**, **Bashore TM**, **Dweik R**, **Krasuski RA.** Impact of diabetes in patients with pulmonary hypertension. *Pulm Circ* 5: 117–123, 2015. doi:10.1086/679705.
4. **Luongo F**, **Miotti C**, **Scoccia G**, **Papa S**, **Manzi G**, **Cedrone N**, **Toto F**, **Malerba C**, **Papa G**, **Caputo A**, **Manguso G**, **Adamo F**, **Carmine DV**, **Badagliacca R.** Future perspective in diabetic patients with pre- and post-capillary pulmonary hypertension. *Heart Fail Rev* 28: 745–755, 2023. doi:10.1007/s10741-021-10208-4.
5. **Breyer MK**, **Spruit MA**, **Hanson CK**, **Franssen FM**, **Vanfleteren LE**, **Groenen MT**, **Bruijnzeel PL**, **Wouters EF**, **Rutten EP.** Prevalence of metabolic syndrome in COPD patients and its consequences. *PLoS One* 9: e98013, 2014. doi:10.1371/journal.pone.0098013.
6. **Kim YJ**, **Park JW**, **Kyung SY**, **Lee SP**, **Chung MP**, **Kim YH**, **Lee JH**, **Kim YC**, **Ryu JS**, **Lee HL**, **Park CS**, **Uh ST**, **Lee YC**, **Kim KH**, **Chun YJ**, **Park YB**, **Kim DS**, **Jegal Y**, **Lee JH**, **Park MS**, **Jeong SH.** Clinical characteristics of idiopathic pulmonary fibrosis patients with diabetes mellitus: the national survey in Korea from 2003 to 2007. *J Korean Med Sci* 27: 756–760, 2012. doi:10.3346/jkms.2012.27.7.756.
7. **Gribbin J**, **Hubbard R**, **Smith C.** Role of diabetes mellitus and gastro-oesophageal reflux in the aetiology of idiopathic pulmonary fibrosis. *Respir Med* 103: 927–931, 2009. doi:10.1016/j.rmed.2008.11.001.
8. **Gulcan E**, **Bulut I**, **Toker A**, **Gulcan A.** Evaluation of glucose tolerance status in patients with asthma bronchiale. *J Asthma* 46: 207–209, 2009. doi:10.1080/02770900802627302.
9. **Shimoda LA**, **Laurie SS.** Vascular remodeling in pulmonary hypertension. *J Mol Med (Berl)* 91: 297–309, 2013. doi:10.1007/s00109-013-0998-0.
10. **Huetsch JC**, **Suresh K**, **Shimoda LA.** Regulation of smooth muscle cell proliferation by NADPH oxidases in pulmonary hypertension. *Antioxidants (Basel)* 8: 56, 2019. doi:10.3390/antiox8030056.
11. **Hayabuchi Y.** The action of smooth muscle cell potassium channels in the pathology of pulmonary arterial hypertension. *Pediatr Cardiol* 38: 1–14, 2017. doi:10.1007/s00246-016-1491-7.
12. **Smith KA**, **Ayon RJ**, **Tang H**, **Makino A**, **Yuan JX.** Calcium-sensing receptor regulates cytosolic [Ca^{2+}] and plays a major role in the development of pulmonary hypertension. *Front Physiol* 7: 517, 2016. doi:10.3389/fphys.2016.00517.
13. **Zhang S**, **Liu X**, **Ge LL**, **Li K**, **Sun Y**, **Wang F**, **Han Y**, **Sun C**, **Wang J**, **Jiang W**, **Xin Q**, **Xu C**, **Chen Y**, **Chen O**, **Zhang Z**, **Luan Y.** Mesenchymal stromal cell-derived exosomes improve pulmonary hypertension through inhibition of pulmonary vascular remodeling. *Respir Res* 21: 71, 2020. doi:10.1186/s12931-020-1331-4.
14. **Rabinovitch M**, **Guignabert C**, **Humbert M**, **Nicolls MR.** Inflammation and immunity in the pathogenesis of pulmonary arterial hypertension. *Circ Res* 115: 165–175, 2014. doi:10.1161/CIRCRESAHA.113.301141.
15. **Yu Q**, **Chan SY.** Mitochondrial and metabolic drivers of pulmonary vascular endothelial dysfunction in pulmonary hypertension. *Adv Exp Med Biol* 967: 373–383, 2017. doi:10.1007/978-3-319-63245-2_24.
16. **Rhodes CJ**, **Im H**, **Cao A**, **Hennigs JK**, **Wang L**, **Sa S**, **Chen PI**, **Nickel NP**, **Miyagawa K**, **Hopper RK**, **Tojais NF**, **Li CG**, **Gu M**, **Spiekerkoetter E**, **Xian Z**, **Chen R**, **Zhao M**, **Kaschwich M**, **Del Rosario PA**, **Bernstein D**, **Zamanian RT**, **Wu JC**, **Snyder MP**, **Rabinovitch M.** RNA sequencing analysis detection of a novel pathway of endothelial dysfunction in pulmonary arterial hypertension. *Am J Respir Crit Care Med* 192: 356–366, 2015. doi:10.1164/rccm.201408-1528OC.
17. **Si R**, **Zhang Q**, **Cabrera JTO**, **Zheng Q**, **Tsuji-Hosokawa A**, **Watanabe M**, **Hosokawa S**, **Xiong M**, **Jain PP**, **Ashton AW**, **Yuan JX**, **Wang J**, **Makino A.** Chronic hypoxia decreases endothelial connexin 40, attenuates endothelium-dependent hyperpolarization-mediated relaxation in small distal pulmonary arteries, and leads to pulmonary hypertension. *J Am Heart Assoc* 9: e018327, 2020. doi:10.1161/JAHA.120.018327.
18. **Voelkel NF**, **Gomez-Arroyo J**, **Abbate A**, **Bogaard HJ**, **Nicolls MR.** Pathobiology of pulmonary arterial hypertension and right ventricular failure. *Eur Respir J* 40: 1555–1565, 2012. doi:10.1183/09031936.00046612.

19. **Huetsch JC**, **Suresh K**, **Bernier M**, **Shimoda LA.** Update on novel targets and potential treatment avenues in pulmonary hypertension. *Am J Physiol Lung Cell Mol Physiol* 311: L811–L831, 2016. doi:10.1152/ajplung.00302.2016.
20. **Fedorowicz A**, **Buczek E**, **Mateuszuk L**, **Czarnowska E**, **Sitek B**, **Jasztal A**, **Chmura-Skirlinska A**, **Dib M**, **Steven S**, **Daiber A**, **Chlopicki S.** Comparison of pulmonary and systemic NO- and PGI2-dependent endothelial function in diabetic mice. *Oxid Med Cell Longev* 2018: 4036709, 2018. doi:10.1155/2018/4036709.
21. **Shu LP**, **Zhang RH**, **Cai YH**, **Zhou JB**, **Yang JK**, **Qi L.** Maternal diabetes mellitus and persistent pulmonary hypertension of the newborn: accumulated evidence from observational studies. *Can J Diabetes* 44: 327–334 e323, 2020. doi:10.1016/j.jcjd.2019.10.002.
22. **Moral-Sanz J**, **Moreno L**, **Cogolludo A**, **Perez-Vizcaino F.** Pulmonary vascular function in insulin resistance and diabetes. *Curr Vasc Pharmacol* 12: 473–482, 2014. doi:10.2174/15701611126661404232228 08.
23. **Nundlall N**, **Playford D**, **Strange G**, **Davis TME**, **Davis WA.** Prevalence, incidence and associates of pulmonary hypertension complicating type 2 diabetes: insights from the fremantle diabetes study phase 2 and national echocardiographic database of Australia. *J Clin Med* 10: 4503, 2021. doi:10.3390/jcm10194503.
24. **Trammell AW**, **Hemnes AR**, **Tseng V**, **Shah AJ**, **Phillips LS**, **Hart CM.** Influence of body weight and diabetes mellitus in patients with pulmonary hypertension. *Am J Cardiol* 134: 130–137, 2020. doi:10.1016/j.amjcard.2020.07.062.
25. **Gallini JW**, **Benkeser D**, **Cui X**, **Shah AJ**, **Phillips LS**, **Hemnes AR**, **Hart CM**, **Trammell AW.** Pulmonary hypertension: a new vascular complication of diabetes? *Chest* 161: 803–806, 2022. doi:10.1016/j.chest.2021.09.005.
26. **Jonas K**, **Kurzyna M**, **Mroczek E**, **Chrzanowski L**, **Mularek-Kubzdela T**, **Skoczylas I**, **Blaszczak P**, **Grzesk G**, **Mizia-Stec K**, **Kusmierczyk B**, **Kaminski K**, **Lewicka E**, **Peregud-Pogorzelska M**, **Tomaszewski M**, **Jachec W**, **Gasior Z**, **Pawlak A**, **Ryczek R**, **Pruszczyk P**, **Doboszynska A**, **Widejko-Pietkiewicz K**, **Zablocka W**, **Waligora M**, **Kopec G.** Impact of diabetes mellitus on disease severity and patient survival in idiopathic pulmonary arterial hypertension: data from the Polish multicentre registry (BNP-PL). *Cardiovasc Diabetol* 22: 177, 2023. doi:10.1186/s12933-023-01885-6.
27. **Bagheri M**, **Agrawal V**, **Annis J**, **Shi M**, **Ferguson JF**, **Freiberg MS**, **Mosley JD**, **Brittain EL.** Genetics of pulmonary pressure and right ventricle stress identify diabetes as a causal risk factor. *J Am Heart Assoc* 12: e029190, 2023. doi:10.1161/JAHA.122.029190.
28. **Whitaker ME**, **Nair V**, **Sinari S**, **Dherange PA**, **Natarajan B**, **Trutter L**, **Brittain EL**, **Hemnes AR**, **Austin ED**, **Patel K**, **Black SM**, **Garcia JGN**, **Yuan Md Ph DJ**, **Vanderpool RR**, **Rischard F**, **Makino A**, **Bedrick EJ**, **Desai AA.** Diabetes mellitus associates with increased right ventricular afterload and remodeling in pulmonary arterial hypertension. *Am J Med* 131: 702.e7–702.e13, 2018. doi:10.1016/j.amjmed.2017.12.046.
29. **Moral-Sanz J**, **Lopez-Lopez JG**, **Menendez C**, **Moreno E**, **Barreira B**, **Morales-Cano D**, **Escolano L**, **Fernandez-Segoviano P**, **Villamor E**, **Cogolludo A**, **Perez-Vizcaino F**, **Moreno L.** Different patterns of pulmonary vascular disease induced by type 1 diabetes and moderate hypoxia in rats. *Exp Physiol* 97: 676–686, 2012. doi:10.1113/expphysiol.2011.062257.
30. **Lopez YLG**, **Tepox Galicia AY**, **Atonal Flores F**, **Flores Hernandez J**, **Perez Vizcaino F**, **Villa Mancera AE**, **Miguel GG**, **Reynoso Palomar A.** Echocardiographic follow-up to right ventricular modifications in secondary pulmonary hypertension to diabetes in rats. *Clin Exp Hypertens* 43: 242–253, 2021. doi:10.1080/10641963.2020.1860077.
31. **Morales-Cano D**, **Callejo M**, **Barreira B**, **Mondejar-Parreno G**, **Esquivel-Ruiz S**, **Ramos S**, **Martin MA**, **Cogolludo A**, **Moreno L**, **Perez-Vizcaino F.** Elevated pulmonary arterial pressure in Zucker diabetic fatty rats. *PLoS One* 14: e0211281, 2019. doi:10.1371/journal.pone.0211281.
32. **Lopez-Lopez JG**, **Moral-Sanz J**, **Frazziano G**, **Gomez-Villalobos MJ**, **Flores-Hernandez J**, **Monjaraz E**, **Cogolludo A**, **Perez-Vizcaino F.** Diabetes induces pulmonary artery endothelial dysfunction by NADPH oxidase induction. *Am J Physiol Lung Cell Mol Physiol* 295: L727–L732, 2008. doi:10.1152/ajplung.90354.2008.
33. **Pan M**, **Han Y**, **Si R**, **Guo R**, **Desai A**, **Makino A.** Hypoxia-induced pulmonary hypertension in type 2 diabetic mice. *Pulm Circ* 7: 175–185, 2017. doi:10.1086/690206.
34. **Cividini F**, **Scott BT**, **Suarez J**, **Casteel DE**, **Heinz S**, **Dai A**, **Diemer T**, **Suarez JA**, **Benner CW**, **Ghassemian M**, **Dillmann WH.** Ncor2/PPARα-dependent upregulation of MCUb in the type 2 diabetic heart impacts cardiac metabolic flexibility and function. *Diabetes* 70: 665–679, 2021. doi:10.2337/db20-0779.
35. **Franko A**, **Neschen S**, **Rozman J**, **Rathkolb B**, **Aichler M**, **Feuchtinger A**, **Brachthauser L**, **Neff F**, **Kovarova M**, **Wolf E**, **Fuchs H**, **Haring HU**, **Peter A**, **Hrabe de Angelis M.** Bezafibrate ameliorates diabetes via reduced steatosis and improved hepatic insulin sensitivity in diabetic TallyHo mice. *Mol Metab* 6: 256–266, 2017. doi:10.1016/j.molmet.2016.12.007.
36. **Kim JH**, **Sen S**, **Avery CS**, **Simpson E**, **Chandler P**, **Nishina PM**, **Churchill GA**, **Naggert JK.** Genetic analysis of a new mouse model for non-insulin-dependent diabetes. *Genomics* 74: 273–286, 2001. doi:10.1006/geno.2001.6569.
37. **Si R**, **Zhang Q**, **Tsuji-Hosokawa A**, **Watanabe M**, **Willson C**, **Lai N**, **Wang J**, **Dai A**, **Scott BT**, **Dillmann WH**, **Yuan JX**, **Makino A.** Overexpression of p53 due to excess protein O-GlcNAcylation is associated with coronary microvascular disease in type 2 diabetes. *Cardiovasc Res* 116: 1186–1198, 2020. doi:10.1093/cvr/cvz216.
38. **Cai R**, **Zhang Y**, **Simmering JE**, **Schultz JL**, **Li Y**, **Fernandez-Carasa I**, **Consiglio A**, **Raya A**, **Polgreen PM**, **Narayanan NS**, **Yuan Y**, **Chen Z**, **Su W**, **Han Y**, **Zhao C**, **Gao L**, **Ji X**, **Welsh MJ**, **Liu L.** Enhancing glycolysis attenuates Parkinson's disease progression in models and clinical databases. *J Clin Invest* 129: 4539–4549, 2019. doi:10.1172/JCI129987.
39. **Liberti MV**, **Dai Z**, **Wardell SE**, **Baccile JA**, **Liu X**, **Gao X**, **Baldi R**, **Mehrmohamadi M**, **Johnson MO**, **Madhukar NS**, **Shestov AA**, **Chio IIC**, **Elemento O**, **Rathmell JC**, **Schroeder FC**, **McDonnell DP**, **Locasale JW.** A predictive model for selective targeting of the Warburg effect through GAPDH inhibition with a natural product. *Cell Metab* 26: 648–659.e8, 2017. doi:10.1016/j.cmet.2017.08.017.
40. **Kumagai S**, **Narasaki R**, **Hasumi K.** Glucose-dependent active ATP depletion by koningic acid kills high-glycolytic cells. *Biochem Biophys Res Commun* 365: 362–368, 2008. doi:10.1016/j.bbrc.2007.10.199.
41. **Kim JH**, **Stewart TP**, **Soltani-Bejnood M**, **Wang L**, **Fortuna JM**, **Mostafa OA**, **Moustaid-Moussa N**, **Shoieb AM**, **McEntee MF**, **Wang Y**, **Bechtel L**, **Naggert JK.** Phenotypic characterization of polygenic type 2 diabetes in TALLYHO/JngJ mice. *J Endocrinol* 191: 437–446, 2006. doi:10.1677/joe.1.06647.
42. **Han X**, **Shaligram S**, **Zhang R**, **Anderson L**, **Rahimian R.** Sex-specific vascular responses of the rat aorta: effects of moderate term (intermediate stage) streptozotocin-induced diabetes. *Can J Physiol Pharmacol* 94: 408–415, 2016. doi:10.1139/cjpp-2015-0272.
43. **Si R**, **Cabrera JTO**, **Tsuji-Hosokawa A**, **Guo R**, **Watanabe M**, **Gao L**, **Lee YS**, **Moon JS**, **Scott BT**, **Wang J**, **Ashton AW**, **Rao JN**, **Wang JY**, **Yuan JX**, **Makino A.** HuR/Cx40 downregulation causes coronary microvascular dysfunction in type 2 diabetes. *JCI Insight* 6: e147982, 2021. doi:10.1172/jci.insight.147982.
44. **Chen WC**, **Park SH**, **Hoffman C**, **Philip C**, **Robinson L**, **West J**, **Grunig G.** Right ventricular systolic pressure measurements in combination with harvest of lung and immune tissue samples in mice. *J Vis Exp* 71: e50023, 2013. doi:10.3791/50023.
45. **Lu H**, **Forbes RA**, **Verma A.** Hypoxia-inducible factor 1 activation by aerobic glycolysis implicates the Warburg effect in carcinogenesis. *J Biol Chem* 277: 23111–23115, 2002. doi:10.1074/jbc.M202487200.
46. **Benson L**, **Brittain EL**, **Pugh ME**, **Austin ED**, **Fox K**, **Wheeler L**, **Robbins IM**, **Hemnes AR.** Impact of diabetes on survival and right ventricular compensation in pulmonary arterial hypertension. *Pulm Circ* 4: 311–318, 2014. doi:10.1086/675994.
47. **Tan JS**, **Yang Y**, **Wang J**, **Wang Y**, **Lv T**, **Shu Y**, **Xu W**, **Chong L.** Diabetes mellitus, glycemic traits, SGLT2 inhibition, and risk of pulmonary arterial hypertension: a Mendelian randomization study. *Biosci Trends* 18: 94–104, 2024. doi:10.5582/bst.2024.01006.
48. **Wang Z**, **Yang K**, **Zheng Q**, **Zhang C**, **Tang H**, **Babicheva A**, **Jiang Q**, **Li M**, **Chen Y**, **Carr SG**, **Wu K**, **Zhang Q**, **Balistrieri A**, **Wang C**, **Song S**, **Ayon RJ**, **Desai AA**, **Black SM**, **Garcia JGN**, **Makino A**, **Yuan JX**, **Lu W**, **Wang J.** Divergent changes of p53 in pulmonary arterial endothelial and smooth muscle cells involved in the development of pulmonary hypertension. *Am J Physiol Lung Cell Mol Physiol* 316: L216–L228, 2019. doi:10.1152/ajplung.00538.2017.
49. **Zheng Q**, **Lu W**, **Yan H**, **Duan X**, **Chen Y**, **Zhang C**, **Luo X**, **Chen J**, **Wang C**, **Liu S**, **Li Y**, **Tang H**, **Rahimi S**, **Rahimi S**, **Yuan JX**, **Zhong N**, **Yang K**, **Wang J.** Established pulmonary hypertension in rats was

reversed by a combination of a HIF-2α antagonist and a p53 agonist. *Br J Pharmacol* 179: 1065–1081, 2022. doi:10.1111/bph.15696.

50. **Wakasugi T**, **Shimizu I**, **Yoshida Y**, **Hayashi Y**, **Ikegami R**, **Suda M**, **Katsuumi G**, **Nakao M**, **Hoyano M**, **Kashimura T**, **Nakamura K**, **Ito H**, **Nojiri T**, **Soga T**, **Minamino T.** Role of smooth muscle cell p53 in pulmonary arterial hypertension. *PLoS One* 14: e0212889, 2019. doi:10.1371/journal.pone.0212889.
51. **Breault NM**, **Wu D**, **Dasgupta A**, **Chen KH**, **Archer SL.** Acquired disorders of mitochondrial metabolism and dynamics in pulmonary arterial hypertension. *Front Cell Dev Biol* 11: 1105565, 2023. doi:10.3389/fcell.2023.1105565.
52. **Xu W**, **Janocha AJ**, **Erzurum SC.** Metabolism in pulmonary hypertension. *Annu Rev Physiol* 83: 551–576, 2021. doi:10.1146/annurev-physiol-031620-123956.
53. **Zhao L**, **Ashek A**, **Wang L**, **Fang W**, **Dabral S**, **Dubois O**, **Cupitt J**, **Pullamsetti SS**, **Cotroneo E**, **Jones H**, **Tomasi G**, **Nguyen QD**, **Aboagye EO**, **El-Bahrawy MA**, **Barnes G**, **Howard LS**, **Gibbs JS**, **Gsell W**, **He JG**, **Wilkins MR.** Heterogeneity in lung ^{18}FDG uptake in pulmonary arterial hypertension: potential of dynamic ^{18}FDG positron emission tomography with kinetic analysis as a bridging biomarker for pulmonary vascular remodeling targeted treatments. *Circulation* 128: 1214–1224, 2013. doi:10.1161/CIRCULATIONAHA.113.004136.
54. **Hernandez-Saavedra D**, **Sanders L**, **Freeman S**, **Reisz JA**, **Lee MH**, **Mickael C**, **Kumar R**, **Kassa B**, **Gu S**, **A DA**, **Stenmark KR**, **Tuder RM**, **Graham BB.** Stable isotope metabolomics of pulmonary artery smooth muscle and endothelial cells in pulmonary hypertension and with TGF-beta treatment. *Sci Rep* 10: 413, 2020 [Erratum in *Sci Rep* 10: 4349, 2020]. doi:10.1038/s41598-019-57200-5.
55. **Marsboom G**, **Wietholt C**, **Haney CR**, **Toth PT**, **Ryan JJ**, **Morrow E**, **Thenappan T**, **Bache-Wiig P**, **Piao L**, **Paul J**, **Chen CT**, **Archer SL.** Lung ^{18}F-fluorodeoxyglucose positron emission tomography for diagnosis and monitoring of pulmonary arterial hypertension. *Am J Respir Crit Care Med* 185: 670–679, 2012. doi:10.1164/rccm.201108-1562OC.
56. **Michelakis ED**, **Gurtu V**, **Webster L**, **Barnes G**, **Watson G**, **Howard L**, **Cupitt J**, **Paterson I**, **Thompson RB**, **Chow K**, **O'Regan DP**, **Zhao L**, **Wharton J**, **Kiely DG**, **Kinnaird A**, **Boukouris AE**, **White C**, **Nagendran J**, **Freed DH**, **Wort SJ**, **Gibbs JSR**, **Wilkins MR.** Inhibition of pyruvate dehydrogenase kinase improves pulmonary arterial hypertension in genetically susceptible patients. *Sci Transl Med* 9: eaao4583, 2017. doi:10.1126/scitranslmed.aao4583.
57. **Xu W**, **Koeck T**, **Lara AR**, **Neumann D**, **DiFilippo FP**, **Koo M**, **Janocha AJ**, **Masri FA**, **Arroliga AC**, **Jennings C**, **Dweik RA**, **Tuder RM**, **Stuehr DJ**, **Erzurum SC.** Alterations of cellular bioenergetics in pulmonary artery endothelial cells. *Proc Natl Acad Sci USA* 104: 1342–1347, 2007. doi:10.1073/pnas.0605080104.
58. **Cao Y**, **Zhang X**, **Wang L**, **Yang Q**, **Ma Q**, **Xu J**, **Wang J**, **Kovacs L**, **Ayon RJ**, **Liu Z**, **Zhang M**, **Zhou Y**, **Zeng X**, **Xu Y**, **Wang Y**, **Fulton DJ**, **Weintraub NL**, **Lucas R**, **Dong Z**, **Yuan JX**, **Sullivan JC**, **Meadows L**, **Barman SA**, **Wu C**, **Quan J**, **Hong M**, **Su Y**, **Huo Y.** PFKFB3-mediated endothelial glycolysis promotes pulmonary hypertension. *Proc Natl Acad Sci USA* 116: 13394–13403, 2019. doi:10.1073/pnas.1821401116.
59. **Caruso P**, **Dunmore BJ**, **Schlosser K**, **Schoors S**, **Dos Santos C**, **Perez-Iratxeta C**, **Lavoie JR**, **Zhang H**, **Long L**, **Flockton AR**, **Frid MG**, **Upton PD**, **D'Alessandro A**, **Hadinnapola C**, **Kiskin FN**, **Taha M**, **Hurst LA**, **Ormiston ML**, **Hata A**, **Stenmark KR**, **Carmeliet P**, **Stewart DJ**, **Morrell NW.** Identification of microRNA-124 as a major regulator of enhanced endothelial cell glycolysis in pulmonary arterial hypertension via PTBP1 (polypyrimidine tract binding protein) and pyruvate kinase M2. *Circulation* 136: 2451–2467, 2017. doi:10.1161/CIRCULATIONAHA.117.028034.
60. **Plecita-Hlavata L**, **Tauber J**, **Li M**, **Zhang H**, **Flockton AR**, **Pullamsetti SS**, **Chelladurai P**, **D'Alessandro A**, **El Kasmi KC**, **Jezek P**, **Stenmark KR.** Constitutive reprogramming of fibroblast mitochondrial metabolism in pulmonary hypertension. *Am J Respir Cell Mol Biol* 55: 47–57, 2016. doi:10.1165/rcmb.2015-0142OC.
61. **D'Alessandro A**, **El Kasmi KC**, **Plecita-Hlavata L**, **Jezek P**, **Li M**, **Zhang H**, **Gupte SA**, **Stenmark KR.** Hallmarks of pulmonary hypertension: mesenchymal and inflammatory cell metabolic reprogramming. *Antioxid Redox Signal* 28: 230–250, 2018. doi:10.1089/ars.2017.7217.
62. **Vestergaard H**, **Bjorbaek C**, **Hansen T**, **Larsen FS**, **Granner DK**, **Pedersen O.** Impaired activity and gene expression of hexokinase II in muscle from non-insulin-dependent diabetes mellitus patients. *J Clin Invest* 96: 2639–2645, 1995. doi:10.1172/JCI118329.
63. **Pan M**, **Han Y**, **Basu A**, **Dai A**, **Si R**, **Willson C**, **Balistrieri A**, **Scott BT**, **Makino A.** Overexpression of hexokinase 2 reduces mitochondrial calcium overload in coronary endothelial cells of type 2 diabetic mice. *Am J Physiol Cell Physiol* 314: C732–C740, 2018. doi:10.1152/ajpcell.00350.2017.
64. **Wang H**, **Wang M**, **Yang X**, **Xu X**, **Hao Q**, **Yan A**, **Hu M**, **Lobinski R**, **Li H**, **Sun H.** Antimicrobial silver targets glyceraldehyde-3-phosphate dehydrogenase in glycolysis of *E. coli*. *Chem Sci* 10: 7193–7199, 2019. doi:10.1039/c9sc02032b.